

# Effect of vacuum sintering conditions on the properties of $Y_3Al_5O_{12} : Ce$ luminescent ceramics

Lyudmila V. Tarala<sup>1</sup>, Alexander A. Kravtsov<sup>1</sup>, Oleg M. Chapura<sup>1</sup>, Vitaly A. Tarala<sup>1</sup>, Dmitry S. Vakalov<sup>1</sup>, Fedor F. Malyavin<sup>1</sup>, Sergey V. Kuznetsov<sup>2,3</sup>, Viacheslav A. Lapin<sup>1</sup>, Lev V. Kozhitov<sup>4</sup>, Alena V. Popkova<sup>5</sup>

<sup>1</sup> North Caucasian Federal University, 1 Pushkin Str., Stavropol 355017, Russian Federation

<sup>2</sup> Prokhorov General Physics Institute of the Russian Academy of Sciences, 38 Vavilov Str., Moscow 119991, Russian Federation

<sup>3</sup> Kazan Federal University, 18 Kremlyovskaya Str., Kazan 420008, Russian Federation

<sup>4</sup> National University of Science and Technology MISiS, 4-1 Leninsky Ave., Moscow 119049, Russian Federation

<sup>5</sup> JSC "Research Institute NPO" LUCH", 24 Zheleznodorozhnaya Str., Podolsk 142103, Russian Federation

Corresponding author: Alexander A. Kravtsov (sanya-kravtsov@ya.ru)

Received 5 September 2022 ♦ Accepted 17 September 2022 ♦ Published 20 October 2022

**Citation:** Tarala LV, Kravtsov AA, Chapura OM, Tarala VA, Vakalov DS, Malyavin FF, Kuznetsov SV, Lapin VA, Kozhitov LV, Popkova AV (2022) Effect of vacuum sintering conditions on the properties of  $Y_3Al_5O_{12} : Ce$  luminescent ceramics. *Modern Electronic Materials* 8(3): 123–130. <https://doi.org/10.3897/j.moem.8.3.98706>

## Abstract

The aim of this work was to study the effect of vacuum sintering conditions and cerium concentration on the optical, luminescent and thermal properties of yttrium-aluminum garnet based ceramics doped with  $Ce^{3+}$  cations. Series of ceramic powders were synthesized and samples of luminescent ceramics having the composition  $Y_{3-x}Ce_xAl_5O_{12}$  were synthesized where  $x$  was in the range 0.01 to 0.025 f.u. We show that the phase composition and grain size distribution of the ceramic powders do not depend on cerium concentration. Without sintering additives, an increase in vacuum sintering temperature from 1675 to 1800 °C leads to an increase in the optical transmittance of luminescent ceramic specimens from 5 to 55% at a 540 nm wavelength and an increase in the thermal conductivity of the samples from 8.4 to 9.5 W/(m · K). It was found that an increase in cerium concentration leads to a shift of the luminescent band peak from 535 to 545 nm where as the width of the luminescent band decreases with an increase in vacuum sintering temperature from 1675 to 1725 °C.

## Keywords

YAG : Ce, luminescence, ceramics vacuum sintering, activator concentration, optical properties

## 1. Introduction

White light-emitting diodes (WLED) due to their higher electrical efficiency as compared with that of luminescent lamps [1, 2] are currently widely used in a number of illumination systems [3, 4]. Blue radiation generated in these

devices by the InGaN-based LED [5, 6] is converted to white light with the use of phosphors [7–9]. Yttrium-aluminum garnet doped with cerium cations (YAG : Ce) is considered as one of the most efficient phosphors [10].

In most of white LED devices for household use, the phosphor is applied onto the blue LED in the form of a

compound. A technical obstacle to increasing the brightness of WLED is the instability of the luminescent compound in the form of YAG:Ce phosphor powder blended with an organic binder. Due to the low thermal conductivity of the composite coating, increasing the energy emitted by the LED leads to WLED degradation and hence to a decrease in the light output and a change in the chromatic coordinates of the device [10–12]. This problem can be solved by replacing composite coatings with luminescent ceramics [10–13]. Due to their higher thermal stability and lower temperature sensitivity as compared with those of phosphor layers, luminescent ceramics exhibit higher light conversion efficiency [14]. After the introduction of commercially available high-power blue semiconductor lasers the requirements to the thermal properties of light converters strengthened, and it became possible to develop ultra-bright white sources [14]. It should also be noted that the demand for ultra-bright white sources exists in the automotive, aircraft, shipbuilding, and mining industries.

The aim of this work was to study the effect of vacuum sintering conditions and cerium concentration on the optical, luminescent and thermal properties of yttrium-aluminum garnet-based ceramics doped with cerium cations.

To this end, ceramic powders of yttrium-aluminum garnet with different cerium concentrations were synthesized. The cerium concentration range was chosen on the basis of earlier investigation results [15] and corresponded to the YAG:Ce compositions exhibiting the strongest luminescence among ceramic powders synthesized in air.

## 2. Experimental

The following reactants were used for the synthesis of ceramic powders: aqueous ammonia (25%, ultrahigh purity, SigmaTech, Russia), aluminum chloride hexahydrate (99%, AcrosOrganics, Belgium), cerium nitrate hexahydrate (99%, Vecton, Russia), yttrium chloride hexahydrate (99%, ChemicalPoint, Germany), ammonia sulfate (99%, Stavreachim, Russia), isopropyl alcohol (99.7%, Khimprom Ltd., Russia).

The ceramic powders having the composition  $Y_{3-x}Ce_xAl_5O_{12}$  ( $x = 0.01, 0.0125, 0.015, 0.0175, 0.02, 0.0225$  and  $0.025$ ) were synthesized by spraying a concentrated solution of cerium, aluminum and yttrium salts into a 25% solution of ammonia taken in a six-fold excess and ammonia sulfate (0.45 M). The precipitate was washed with an ammonia sulfate solution (0.045 M). The washed precipitate was dried in a drying chamber at 60 °C for 15 h. The dried precipitate was air-annealed in corundum crucibles in a Nabertherm 08/18 furnace at 1200 °C for 2 h. We did not blend the ceramic powders with any sintering additives in order to avoid their potential influence on the conversion of exciting energy to  $Ce^{3+}$  cation luminescence. The synthesized ceramic powders were uniaxially pressed at 50 MPa to ceramic green bodies in the form of 15 mm diam. 4 mm thick discs. The

ceramic samples were sintered in a vacuum furnace at six different temperatures, i.e., 1675, 1700, 1725, 1750, 1775 and 1800 °C, the isothermal exposure duration being 10 h. After vacuum sintering for oxygen vacancy removal the ceramic specimens were air-annealed at 1450 °C for 10 h in a high-temperature Nabertherm 08/18 furnace (Germany).

The ceramic disc samples were mechanically ground to the same thickness ( $1 \pm 0.01$  mm) and polished to high luster on a QPol-250 machine (Germany).

The light transmittance spectra were recorded in the 200 to 900 nm region using an SF-56 spectrophotometer (JSC OKB Spectr, Russia).

The phase composition of the ceramic powders was studied using X-ray diffraction (Empyrean, Panalytical, Netherlands) with a copper cathode X-ray tube ( $CuK_{\alpha 1}$ ,  $\lambda = 0.15406$  nm) in a  $2\theta$  range of 10 to 90 arc deg at a 0.01 deg step and a 0.7 deg/min scanning speed. The constituent phases were identified using the HighscorePlus software with the ICDD PDF-2 database.

The micrographs of the ceramic powders were made under a scanning electron microscope (FESEM, LM Mira 3, Tescan, Czech Republic).

The temperature conductivity and the isobaric specific heat capacity of the ceramics were measured with an LFA 467 HyperFlash laser flash device (Netzsch, Germany) with a pyroceramic reference. The thermal conductivity was calculated using the following equation:

$$\chi = gC_p r,$$

where  $\chi$  is the thermal conductivity,  $g$  is the temperature conductivity,  $C_p$  is the isobaric specific heat capacity and  $r$  is the density.

The density of the samples was measured by hydrostatic weighing on an HR-250AZG analytical balance with a hydrostatic weighing attachment.

The luminescence spectra were recorded using an SFL-MDR spectrophotometer (JSC OKB Spectr, Russia).

## 3. Results and discussion

Figure 1 shows a micrograph illustrating the typical morphology of the YAG ceramic powders synthesized by chemical precipitation [16–18]. Analysis of the SEM micrographs showed that the ceramic powders consist of agglomerates of primary particles sized about 150 nm. The data summarized in Table 1 suggest that all the  $Y_{3-x}Ce_xAl_5O_{12}$  powder samples had close grain size distributions.

Identification of the X-ray diffraction patterns (Fig. 2) showed that the only constituent phase in all the synthesized powders was yttrium-aluminum garnet. No other phases were found. Evaluation of the crystal lattice parameters ( $a$ ) of the  $Y_{3-x}Ce_xAl_5O_{12}$  powders did not reveal any significant differences between the samples. The difference of the  $a$  parameters of the samples was within the

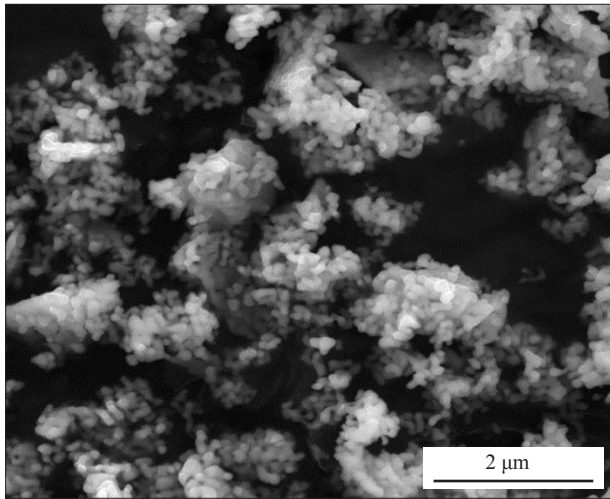


**Figure 1.** Micrograph of  $Y_{3-x}Ce_xAl_5O_{12}$  ceramic powder ( $x = 0.0175$ )

**Table 1.** Grain size distribution in  $Y_{3-x}Ce_xAl_5O_{12}$  ceramic powders

$Y_{3-x}Ce_xAl_5O_{12}$	$D_{10}$ ( $\mu\text{m}$ )	$D_{50}$ ( $\mu\text{m}$ )	$D_{90}$ ( $\mu\text{m}$ )
$x = 0.01$	0.395	2.204	6.345
$x = 0.0125$	0.419	2.447	6.543
$x = 0.015$	0.405	2.296	6.362
$x = 0.0175$	0.409	2.415	6.495
$x = 0.02$	0.407	2.357	6.564
$x = 0.0225$	0.412	2.228	6.356
$x = 0.025$	0.413	2.306	6.335

experimental error ( $\pm 0.00025$  nm). The calculated  $a$  values ( $1.2014 \pm 0.00025$  nm) were in a good agreement with earlier data [15] for single-phase YAG : Ce solid solutions samples of having comparable compositions. The size of coherent scattering regions ( $63 \pm 3$  nm) suggested that the synthesized samples were crystalline powders.

The fact that the ceramic powders had similar grain size distributions and phase compositions allows one to ignore in further analysis the effect of these parameters on the properties of the luminescent ceramics synthesized by vacuum sintering.

Figure 3 *a* shows photographs of  $Y_{3-x}Ce_xAl_5O_{12}$  ceramic samples after vacuum sintering and subsequent annealing in air. For a series of samples containing 0.0175 f.u. Ce it can be seen (Fig. 3 *b*), that an increase in the sintering temperature leads to an increase in the transmittance in the 400–500 nm region. The strong absorption in the 400–500 nm region is caused by photon absorption by  $Ce^{3+}$  cations [15]. The low transmittance of the ceramic samples sintered at 1775–1800 °C is due to the absence of a sintering additive in the ceramic powder.

The 540 nm wavelength was chosen for qualitative estimation of specimen transparency since this wavelength is beyond the absorption bands of extrinsic or intrinsic defects and close to the luminescence spectrum peaks of typical YAG : Ce solid solutions. Analysis of 540 nm transmittance as a function of cerium concentration ( $x$ ) and vacuum sintering temperature ( $T$ ) (Fig. 3 *c*) shows that the transparency of the ceramics increases with an increase in  $T$  and a decrease in  $x$ .

It should be noted that the transparency of the ceramics depends on the concentration of residual pores which act as light scattering centers. The light transmittance

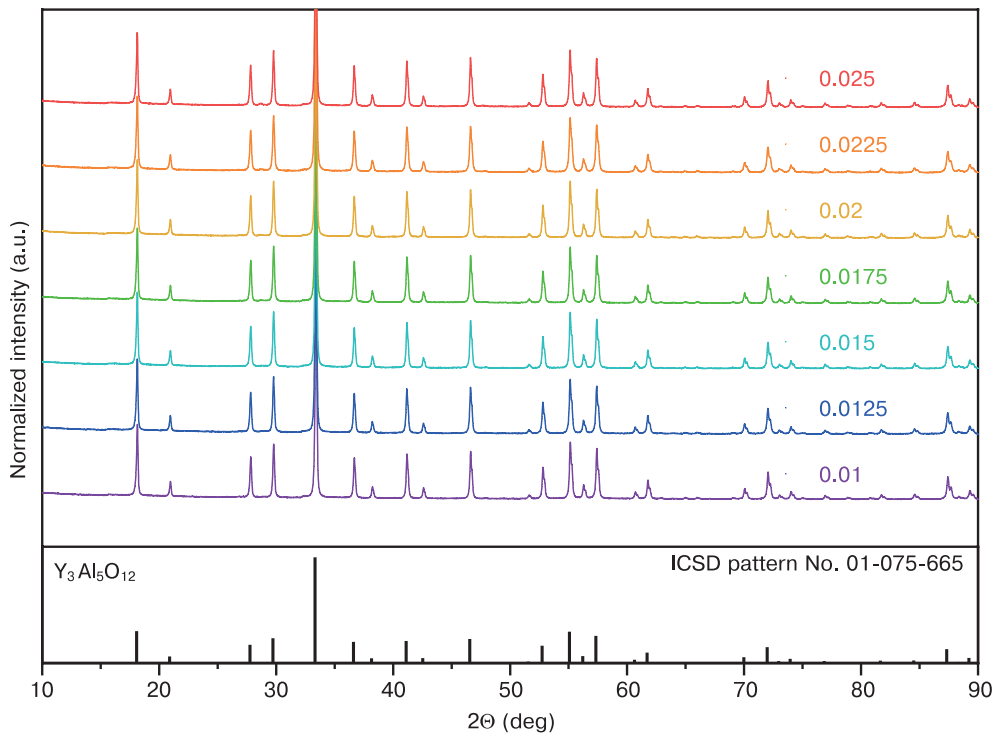


**Figure 2.** X-ray diffraction patterns of  $Y_{3-x}Ce_xAl_5O_{12}$  ceramic powders

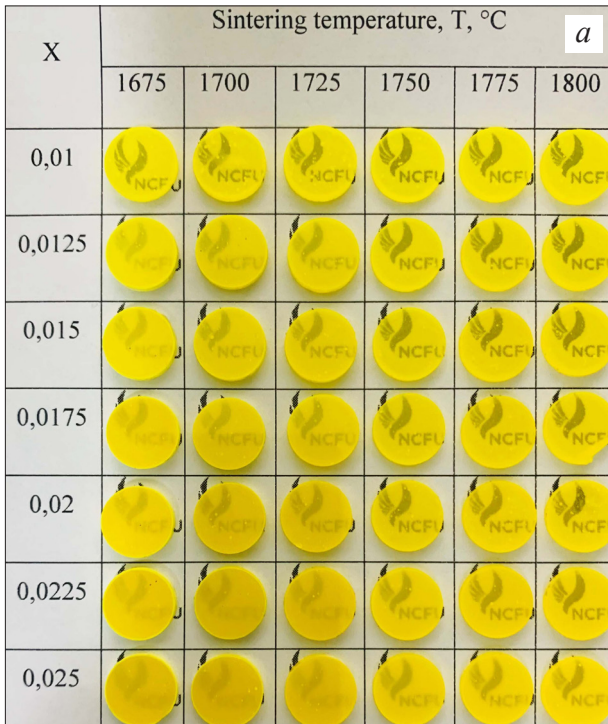
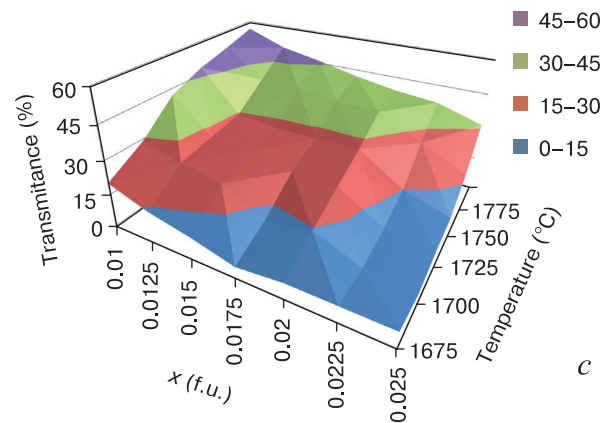
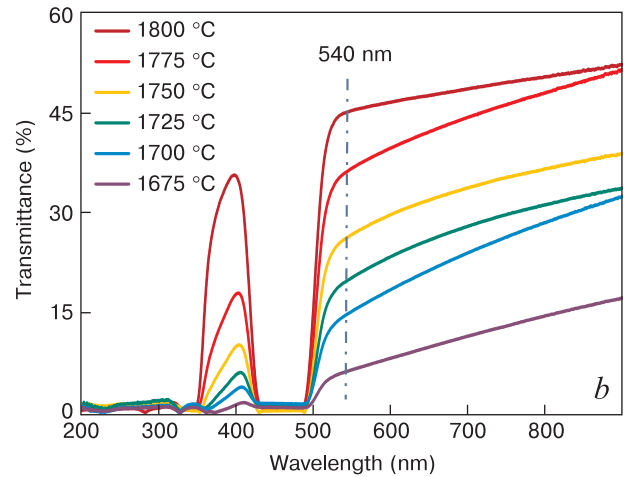


**Figure 3.** (a) Photographs of  $Y_{3-x}Ce_xAl_5O_{12}$  ceramic samples; (b) transmittance spectra of  $Y_{3-x}Ce_xAl_5O_{12}$  series of samples with a 0.0175 f.u. cerium content; (c) transmittance of  $Y_{3-x}Ce_xAl_5O_{12}$  ceramic samples at a 540 nm wavelength as a function of cerium concentration ( $x$ ) and vacuum sintering temperature ( $T$ )



of pore-free YAG:Ce optical ceramics may be as high as 80% and can achieve values comparable with those of single crystals having the same compositions [16, 19–21].

In our opinion, however, the experimentally observed dependences of the transmittance on cerium concentration and sintering temperature are justified. Ceramic sintering leads to the densification of green bodies as well as ceramic powder nanoparticles and their agglomerates. The rate of this process is controlled by diffusion laws and is therefore temperature-dependent. Thus, sintering is faster at elevated temperatures. Furthermore, high temperatures deliver additional energy for the incorporation of cerium atoms in yttrium sites in the yttrium-aluminum garnet crystal lattice. From the energy viewpoint the incorporation of relatively large  $Ce^{3+}$  cations (0.1143 nm) into the dodecahedral site of the YAG crystal lattice requires more energy than the incorporation of  $Y^{3+}$  cations having an ionic radius of 0.1019 nm.

Therefore, the ceramic samples with low cerium contents undergo more rapid compaction and achieve higher transparency at lower vacuum sintering temperatures as compared with samples having relatively high cerium concentrations.

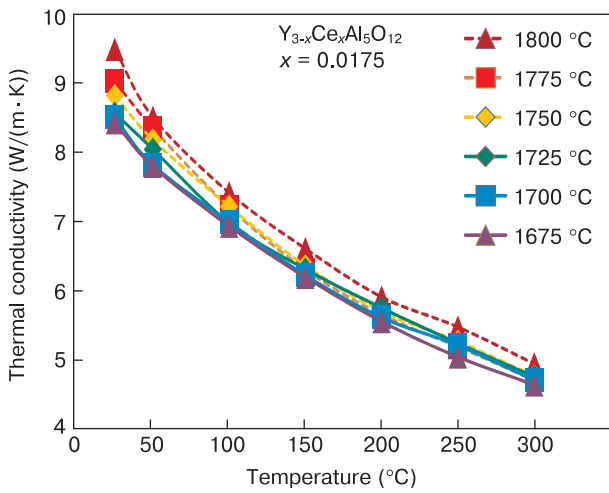
Studies of the thermal conductivity of the ceramic samples with different cerium concentrations at 25 °C did not reveal any significant differences. There is a tendency of increasing the thermal conductivity from 8.4 to 9.5 W/(m·K) with an increase in the vacuum sintering

temperature from 1675 to 1800 °C. Taking into account the increase in the transmittance of the ceramic samples with an increase in temperature one can conclude that the most probable origin of the growth in the thermal conductivity is the reduction of the porosity of the ceramic samples.

Importantly, an increase in the WLED power entails an increase in the energy absorbed by the ceramic converter and hence increasing the thermal conductivity is a necessary condition for the designing of high-power WLED.

Figure 4 shows curves of thermal conductivity as a function of temperature for  $Y_{3-x}Ce_xAl_5O_{12}$  ceramic samples containing 0.0175 f.u. of cerium. These curves are typical of all the series of samples synthesized in this work. It can be seen that the thermal conductivity of the samples decreases by approx. 50% with an increase in temperature from 25 to 300 °C. The decrease in the conductivity is caused by stronger phonon-phonon scattering [22].

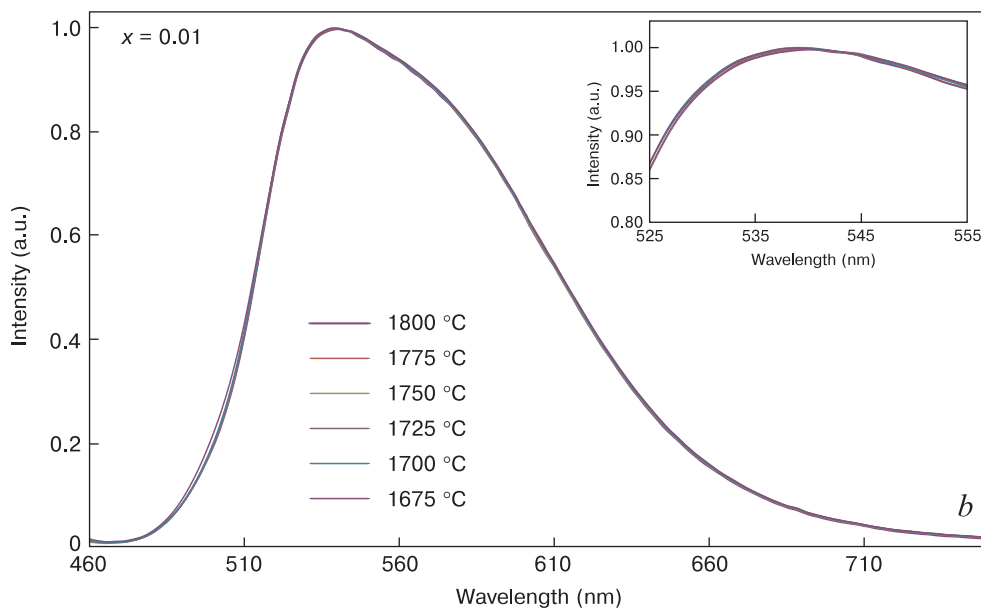
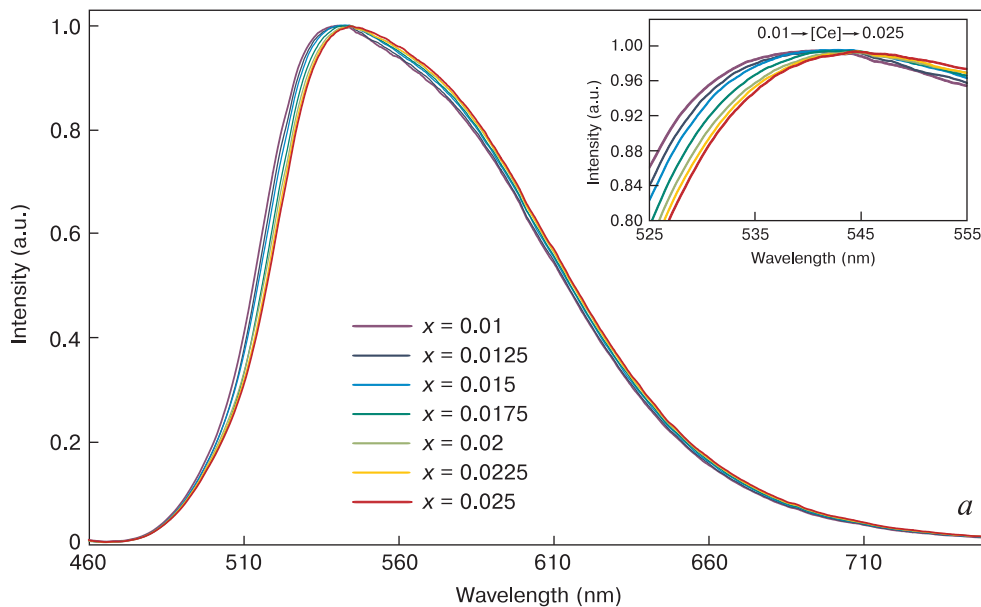
Study of the luminescent properties of the  $Y_{3-x}Ce_xAl_5O_{12}$  samples for 450 nm excitation (Fig. 5) showed that the luminescence peaks are in the 535–545 nm region, these results being in a good agreement with the references [23–26]. The nature of the YAG:Ce luminescence spectra is related to electron energy transitions between the degenerate  $5d$  levels of the excited state and two  $4f$  levels of the main state of the  $Ce^{3+}$  cations [27].



**Figure 4.** Dependences of the thermal conductivity of a series of  $Y_{3-x}Ce_xAl_5O_{12}$  samples with a cerium content of 0.0175 f.u.

The study revealed a slight shift of the spectra with an increase in the cerium concentration from 0.01 to 0.025 f.u. This phenomenon agrees well with earlier data [15] indicating a red shift of the spectra with an increase in cerium concentration from 0.018 to 0.63 f.u.

It is important to note that the positions of the peaks and the shape of the photoluminescence spectra for the samples with the lowest cerium concentration ( $x = 0.01$  f.u.) depended but slightly on the ceramic vacuum sintering temperature (Fig. 5 b). With an increase in the cerium concentration the effect of the sintering temperature on the luminescent properties of the ceramics became stronger. It can be seen from Fig. 5 c that the luminescence spectrum of the sample containing  $x = 0.025$  f.u. cerium sintered at 1675 °C is blue-shifted relative to the spectrum of the sample sintered at 1800 °C. Since the blue shift of the luminescence spectra is caused by a decrease in the  $Ce^{3+}$  concentration, one can easily understand that



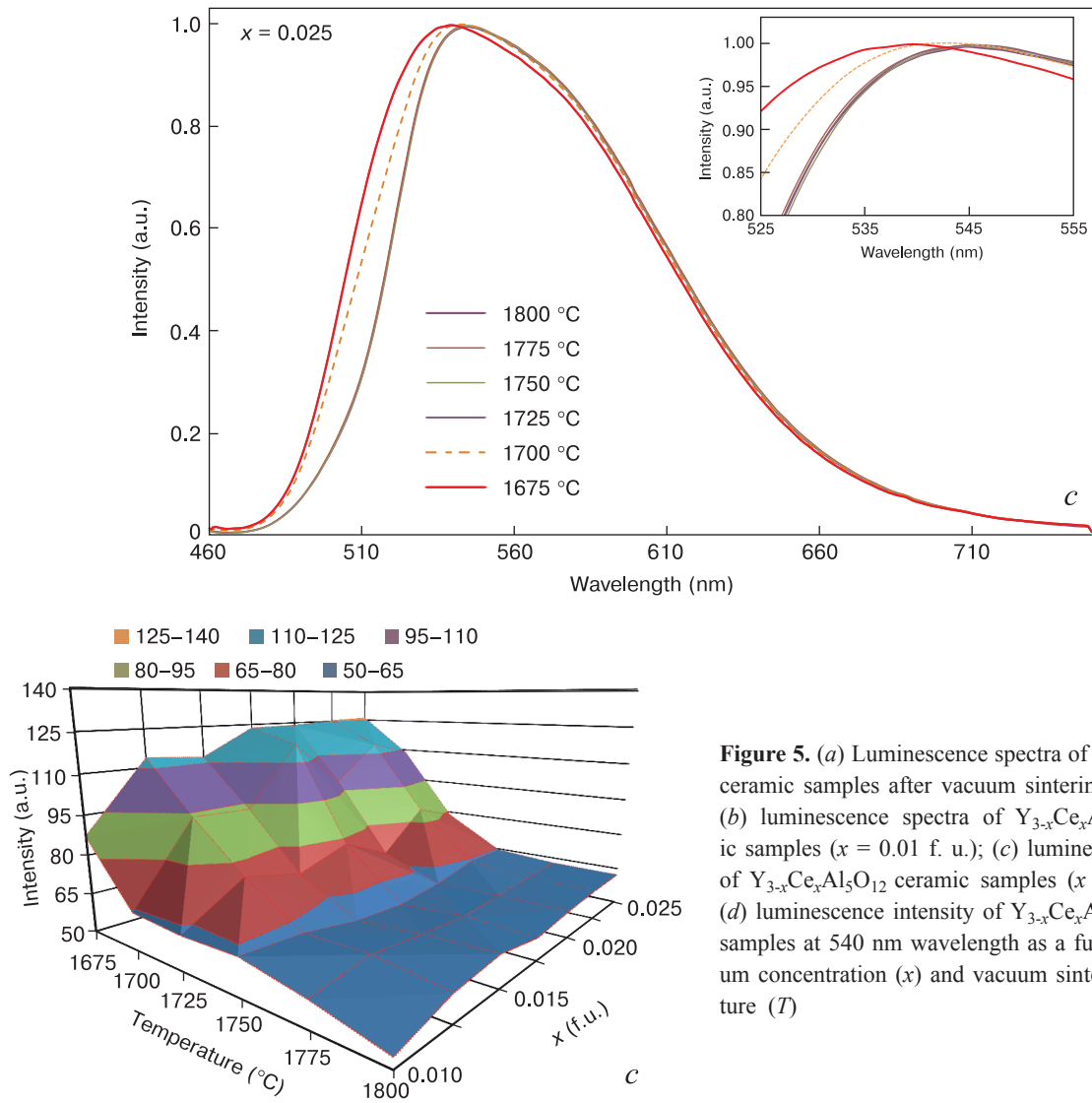


**Figure 5.** (a) Luminescence spectra of  $Y_{3-x}Ce_xAl_5O_{12}$  ceramic samples after vacuum sintering at 1800 °C; (b) luminescence spectra of  $Y_{3-x}Ce_xAl_5O_{12}$  ceramic samples ( $x = 0.01$  f. u.); (c) luminescence spectra of  $Y_{3-x}Ce_xAl_5O_{12}$  ceramic samples ( $x = 0.025$  f.u.); (d) luminescence intensity of  $Y_{3-x}Ce_xAl_5O_{12}$  ceramic samples at 540 nm wavelength as a function of cerium concentration ( $x$ ) and vacuum sintering temperature ( $T$ )

only partial incorporation of  $Ce^{3+}$  cations in the dodecahedral sites of the YAG crystal lattice took place at low vacuum sintering temperatures. The rest of the cations could probably change the oxidation degree from  $Ce^{3+}$  to  $Ce^{4+}$  and localize at ceramic grain boundaries or in the intergranular space. With an increase in temperature, the part of the  $Ce^{3+}$  cations localized in the YAG lattice grew and therefore the luminescent spectrum red-shifted as shown in Fig. 5 c.

Study of the effect of vacuum sintering conditions on the luminescence intensity showed that regardless of cerium concentration the luminescence intensity decreased with an increase in temperature (Fig. 5 d). The greatest changes were observed in the samples synthesized at 1675 to 1750 °C. Note that the luminescence intensity grew in this temperature range with an increase in the cerium concentration. However neither the cerium concentration nor the sintering temperature exerted any significant effect on the luminescence intensity in the 1750 to 1800 °C range.

Although the luminescence intensity increased with a decrease in the vacuum sintering temperature, reducing

the vacuum sintering temperature to below 1675 °C is not expedient since this would further reduce the thermal conductivity of the ceramics. As shown earlier [14], YAG : Ce ceramics with a thermal conductivity of 8.3 W/(m · K) reach the higher limit of light flux of about 400 lm/mm<sup>2</sup> at an excitation power of slightly above 8 W/mm<sup>2</sup> whereas ceramics with a thermal conductivity of 9.6 W/(m · K) excited with a light power of above 10 W/mm<sup>2</sup> can produce a light flux of up to 1200 lm/mm<sup>2</sup>. This large difference in the light flux is accounted for by the strong thermal quenching of luminescence upon heating of low thermal conductivity samples.

Analysis of the experimental results suggests that the experimentally observed dependences (see Fig. 5) can be associated with changes in the optical properties of the ceramics (see Fig. 3). The relatively high luminescence intensity of the samples exhibiting the lowest transmittance is caused by the back-reflection of photons at grain boundaries. Multiple back-reflection events increase the probability of the absorption of excitation radiation quanta by  $Ce^{3+}$  cations and as a result improve the efficiency of light conversion during luminescence. This assumption

was confirmed in an earlier work [28] reporting an increase in the luminescence intensity with an increase in the roughness of YAG : Ce sample surface.

## 4. Conclusion

Experimental studies showed that the luminescence intensity and the peak positions of the luminescence spectra depend on cerium concentration in  $Y_{3-x}Ce_xAl_5O_{12}$  and on vacuum sintering temperature. An increase in vacuum sintering temperature from 1675 to 1800 °C favors the substitution of yttrium cations by cerium cations in high concentrations and leads to an increase in the transmittance of 1 mm thick ceramic samples at a 540 nm wavelength from  $5 \pm 3$  to  $55 \pm 3\%$  and an increase in the thermal conductivity of the ceramics from 8.4 to

9.5 W/(m · K). The luminescence intensity of the ceramics decreases by approx. 2.5 times. In the meantime a decrease in vacuum sintering temperature to below 1700 °C causes broadening of the ceramic luminescence spectra toward the blue region. These results open up an opportunity not only to vary the transparency of YAG : Ce ceramics over a wide range by selecting vacuum sintering temperature and activator concentration but also to efficiently control the luminescence spectrum of the ceramics.

## Acknowledgment

This work was carried out under State Assignment No. 075-01281-22-05 of the North-Caucasus Federal University and employing facilities of the Joint Use Center of the North-Caucasus Federal University.

## References

- Fujii T., Gao Y., Sharma R., Hu E.L., Denbaars S., Nakamura S. Increase in the extraction efficiency of GaN-based light-emitting diodes via surface roughening. *Applied Physics Letters*. 2004; 84(6): 855–857. <https://doi.org/10.1063/1.1645992>
- Narukawa Y., Ichikawa M., Sanga D., Sano M., Mukai T. White light emitting diodes with super-high luminous efficacy. *Journal of Physics D: Applied Physics*. 2010; 43(35): 354002–354003. <https://doi.org/10.1088/0022-3727/43/35/354002>
- Reiter W.L., Stengl G. A blue light emitting diode used as a reference element in scintillation spectrometers. *Nuclear Instruments and Methods*. 1981; 180(1): 105–107.
- Feezell D.F., Speck J., Denbaars S., Nakamura S. Semipolar (20-2-1) InGaN/GaN light-emitting diodes for high-efficiency solid-state lighting. *Journal of Display Technology*. 2013; 9(4): 190–198. <https://doi.org/10.1109/JDT.2012.2227682>
- Nakamura S. The roles of structural imperfections in InGaN-based blue light-emitting diodes and laser diodes. *Science*. 1998; 281(5379): 956–961. <https://doi.org/10.1126/science.281.5379.956>
- Ahmad S., Raushan M.A., Siddiqui M.J. Achievements and perspectives of GaN based light emitting diodes: A critical review. *Proc. 2017 Inter. conf. on trends in electronics and informatics (ICEI), May 11–12, 2017. SCAD College of Engineering and Technology, Tirunelveli, TamilNadu, India*; 2017. P. 224–229. <https://doi.org/10.1109/ICOEI.2017.8300921>
- Guo F., Yuan R., Yang Y.L., Zhang Z.J., Zhao J.T., Lin H. An effective heat dissipation strategy improving efficiency and thermal stability of phosphor-in-glass for high-power WLEDs. *Ceramics International*. 2022; 48(9): 13185–13192. <https://doi.org/10.1016/j.ceramint.2022.01.195>
- Yao Q., Zhang L., Zhang J., Jiang Zh., Sun B., Shao C., Ma Y., Zhou T., Wang K., Zhang L., Chen H., Wang Y. Simple mass-preparation and enhanced thermal performance of Ce: YAG transparent ceramics for high power white LEDs. *Ceramics International*. 2019; 45(5): 6356–6362. <https://doi.org/10.1016/j.ceramint.2018.12.121>
- Liu Y., Su H., Lu Z., Shen Zh., Guo Y., Zhao D., Li Sh., Zhang J., Liu L., Fu H. Energy transfer and thermal stability enhancement in Ce/Cr co-doped  $Al_2O_3$ /YAG eutectic phosphor ceramics for broadband red-emission. *Ceramics International*. 2022; 48(16): 23598–23608. <https://doi.org/10.1016/j.ceramint.2022.05.008>
- Nishiura S., Tanabe S., Fujioka K., Fujimoto Y. Properties of transparent Ce:YAG ceramic phosphors for white LED. *Optical Materials*. 2011; 33(5): 688–691. <https://doi.org/10.1016/j.optmat.2010.06.005>
- Yang C.-C., Chang C.-L., Huang K.-Ch., Taishan L. The yellow ring measurement for the phosphor-converted white LED. *Physics Procedia*. 2011; 19: 182–187. <https://doi.org/10.1016/j.phpro.2011.06.146>
- Nishiura S., Tanabe S., Fujioka K., Fujimoto Y. Preparation and optical properties of transparent Ce:YAG ceramics for high power white LED. *IOP Conference Series: Materials Science and Engineering*. 2009; 1(1): 012031–012036. <https://doi.org/10.1088/1757-8981/1/1/012031>
- Kwon S.B., Choi S.H., Yoo J.H., Jeong S.G., Song Y.-H., Yoon D.H. Synthesis design of  $Y_3Al_5O_{12}$ :  $Ce^{3+}$  phosphor for fabrication of ceramic converter in automotive application. *Optical Materials (Amsterdam)*. 2018; 80: 265–270. <https://doi.org/10.1016/j.optmat.2018.04.037>
- Zhu Q.-Q., Li Sh., Yuan Q., Zhang H., Wang L. Transparent YAG:Ce ceramic with designed low light scattering for high-power blue LED and LD applications. *Journal of the European Ceramic Society*. 2021; 41(1): 735–740. <https://doi.org/10.1016/j.jeurceramsoc.2020.09.006>
- Nakamura H., Shinozaki K., Okumura T., Nomura K. Massive red shift of  $Ce^{3+}$  in  $Y_3Al_5O_{12}$  incorporating super-high content of Ce. *RSC Advances*. 2020; 10(21): 12535–12546. <https://doi.org/10.1039/D0RA01381A>
- Nikova M., Tarala V., Malyavin F.F., Vakalov D., Lapin V.A., Kuleshov D.S., Kravtsov A.I., Chikulina I., Tarala L.V., Evtushenko E.A., Medyanik E.V., Krandievsky S.O., Bogach A.V., Kuznetsov S.V. The scandium impact on the sintering of YAG:Yb ceramics with high optical transmittance. *Ceramics International*. 2021; 47(2): 1772–1784. <https://doi.org/10.1016/j.ceramint.2020.09.003>

17. Kravtsov A., Chikulina I., Tarala V., Vakalov D., Nikova M., Malyavin F.F., Krandievsky S.O., Blinov A., Lapin V.A. Nucleation and growth of YAG: Yb crystallites: A step towards the dispersity control. *Ceramics International*. 2020; 46(18): 28585–28593. <https://doi.org/10.1016/j.ceramint.2020.08.016>
18. Kravtsov A.A., Chikulina I., Tarala V.A., Evtushenko E.A., Nikova M., Tarala V., Malyavin F.F., Vakalov D., Lapin V.A., Kuleshov D.S. Novel synthesis of low-agglomerated YAG:Yb ceramic nanopowders by two-stage precipitation with the use of hexamine. *Ceramics International*. 2019; 45(1): 1273–1282. <https://doi.org/10.1016/j.ceramint.2018.10.010>
19. Tarala V.A., Nikova M., Kuznetsov S.V., Chikulina I., Kravtsov A.I., Vakalov D., Krandievsky S.O., Malyavin F.F., Ambartsumov M., Kozhitov L.V., Mitrofanenko L.M. Synthesis of YAG:Er ceramics and the study of the scandium impact in the dodecahedral and octahedral garnet sites on the Er<sup>3+</sup> energy structure. *Journal of Luminescence*. 2022; 241: 118539–118543. <https://doi.org/10.1016/j.jlumin.2021.118539>
20. Liu Q., Liu J., Li J., Ivanov M.G., Medvedev A., Zeng Y., Jin G., Ba X., Liu W., Jiang B., Pan Y., Guo J. Solid-state reactive sintering of YAG transparent ceramics for optical applications. *Journal of Alloys and Compounds*. 2014; 616: 81–88. <https://doi.org/10.1016/j.jallcom.2014.06.013>
21. Zhang L., Yao Q., Yuan Z., Jiang Zh., Gu L., Sun B., Shao C., Zhou T., Bu W., Wang Y., Chen H. Ammonium citrate assisted surface modification and gel casting of YAG transparent ceramics. *Ceramics International*. 2018; 44(17): 21921–21927. <https://doi.org/10.1016/j.ceramint.2018.08.304>
22. Ramírez-Rico J., Singh M., Zhu D., Martínez Fernández J. High-temperature thermal conductivity of biomorphic SiC/Si ceramics. *Journal of Materials Science*. 2017; 52(17): 10038–10046. <https://doi.org/10.1007/s10853-017-1199-y>
23. Abd H.R., Hassan Z., Alrawi N., Omar A.F., Thahab S.M., Lau Kh.Sh. Rapid synthesis of Ce<sup>3+</sup>:YAG via CO<sub>2</sub> laser irradiation combustion method: Influence of Ce doping and thickness of phosphor ceramic on the performance of a white LED device. *Journal of Solid State Chemistry*. 2021; 294(3): 121866–121877. <https://doi.org/10.1016/j.jssc.2020.121866>
24. Zhang L., Lu Zh., Zhu J., Yang H., Han P., Chen Y., Zhang Q. Citrate sol-gel combustion preparation and photoluminescence properties of YAG:Ce phosphors. *Journal of Rare Earths*. 2012; 30(4): 289–296. [https://doi.org/10.1016/S1002-0721\(12\)60040-4](https://doi.org/10.1016/S1002-0721(12)60040-4)
25. Kravtsov A.A., Chikulina I.S., Vakalov D.S., Chapura O.M., Krandievskii S.O., Devitskii O.V., Lapin V.A. Luminescence of YAG:Ce doped with silver nanoparticles. In: *Physical and chemical aspects of the study of clusters, nanostructures and nanomaterials*. Tver: Izdatel'stvo Tverskogo gosudarstvennogo universiteta; 2021. Iss. 13. P. 220–227. (In Russ.). <https://doi.org/10.26456/pcascnn/2021.13.220>
26. Lukyashin K.E., Ishchenko A.V., Shitov V., Shevelev V., Victorov L.V. Effect of the sintering aids on optical and luminescence properties of Ce:YAG ceramics. *IOP Conference Series: Materials Science and Engineering*. 2019; 525: 012035–012046. <https://doi.org/10.1088/1757-899X/525/1/012035>
27. Abd H.R., Hassan Z., Alrawi N., Almessiere M.A., Omar A.F., Alsultany F.H., Sabah F.A., Osman U.Sh. Effect of annealing time of YAG:Ce<sup>3+</sup> phosphor on white light chromaticity values. *Journal of Electronic Materials*. 2018; 47(2): 1638–1646. <https://doi.org/10.1007/s11664-017-5968-9>
28. Wagner A., Ratzker B., Kalabukhov S., Frage N. Enhanced external luminescence quantum efficiency of ceramic phosphors by surface roughening. *Journal of Luminescence*. 2019; 213: 454–458. <https://doi.org/10.1016/j.jlumin.2019.05.058>